Dual roles of the sixth transmembrane segment of the CFTR chloride channel in gating and permeation

Yonghong Bai,[1,2] Min Li,[1] and Tzyh-Chang Hwang[1,2,3]

[1]Dalton Cardiovascular Research Center, [2]Department of Biological Engineering, and [3]Department of Medical Pharmacology and Physiology, University of Missouri-Columbia, Columbia, MO 65211

Cystic fibrosis transmembrane conductance regulator (CFTR) is the only member of the adenosine triphosphate–binding cassette (ABC) transporter superfamily that functions as a chloride channel. Previous work has suggested that the external side of the sixth transmembrane segment (TM6) plays an important role in governing chloride permeation, but the function of the internal side remains relatively obscure. Here, on a cysless background, we performed cysteine-scanning mutagenesis and modification to screen the entire TM6 with intracellularly applied thiol-specific methanethiosulfonate reagents. Single-channel amplitude was reduced in seven cysteine-substituted mutants, suggesting a role of these residues in maintaining the pore structure for normal ion permeation. The reactivity pattern of differently charged reagents suggests that the cytoplasmic part of TM6 assumes a secondary structure of an α helix, and that reactive sites (341, 344, 345, 348, 352, and 353) reside in two neighboring faces of the helix. Although, as expected, modification by negatively charged reagents inhibits anion permeation, interestingly, modification by positively charged reagents of cysteine thiolates on one face (344, 348, and 352) of the helix affects gating. For I344C and M348C, the open time was prolonged and the closed time was shortened after modification, suggesting that depositions of positive charges at these positions stabilize the open state but destabilize the closed state. For R352C, which exhibited reduced single-channel amplitude, modifications by two positively charged reagents with different chemical properties completely restored the single-channel amplitude but had distinct effects on both the open time and the closed time. These results corroborate the idea that a helix rotation of TM6, which has been proposed to be part of the molecular motions during transport cycles in other ABC transporters, is associated with gating of the CFTR pore.

INTRODUCTION

ATP-binding cassette (ABC) transporters use the energy of ATP binding and hydrolysis to power the active translocation of a broad range of substrates across biological membranes. Their basic architecture comprises two transmembrane domains (TMDs) that form the substrate translocation pathway and two cytoplasmic nucleotide-binding domains (NBDs) that interact with ATP. For the highly conserved NBDs, a common mechanism has emerged wherein ATP binding to the canonical Walker motifs in one NBD recruits the signature sequence of the partner NBD to initiate dimerization of the two NBDs; ATP hydrolysis subsequently disrupts the dimer (for reviews see Higgins and Linton, 2004; Locher, 2009; Rees et al., 2009). In contrast, with regard to TMDs, which must serve diverse functions for different transporters, the molecular determinants of the translocation pathway and the conformational changes associated with the transport cycle remain largely elusive. Recent crystallographic studies, however, do provide evidence for the long-suspected movement of TMDs alternating between the inward-facing and outward-facing configurations for each transport cycle (Ward et al., 2007; Khare et al., 2009).

CFTR, the culprit behind the inherited disease cystic fibrosis, is a unique member of the ABC superfamily in that its two TMDs, each containing six transmembrane segments (TMs) (Fig. 1 A), constitute an ion permeation pathway for the passive Cl^- flow (Riordan et al., 1989; Bear et al. 1992). In addition to the four ABC domains, CFTR contains an intracellular regulatory domain (R domain) with multiple consensus sites, whose phosphorylation by PKA allows ATP to gate the channel (for reviews see Gadsby et al., 2006; Chen and Hwang, 2008; Hwang and Sheppard, 2009). Extensive functional studies together with high-resolution structures of CFTR's two NBDs have provided mechanistic insights into the functional role and possible conformational changes of NBDs in controlling CFTR gating. However, the molecular mechanism for the channel pore in TMDs is not well understood, despite a body of functional

Correspondence to Tzyh-Chang Hwang: hwangt@health.missouri.edu

Abbreviations used in this paper: ABC, ATP-binding cassette; DTT, dithiothreitol; MTS, methanethiosulfonate; MTSEA, 2-amino-ethyl MTS; MTSES, 2-sulfonato-ethyl MTS; MTSET, 2-trimethylammonium-ethyl MTS; NBD, nucleotide-binding domain; TM, transmembrane segment; TMD, transmembrane domain; WT, wild type.

The Rockefeller University Press $30.00
J. Gen. Physiol. Vol. 136 No. 3 293–309
www.jgp.org/cgi/doi/10.1085/jgp.201010480

studies demonstrating that mutations affect ion-permeation properties (Linsdell et al., 1998; Mansoura et al., 1998; McCarty and Zhang, 2001). Systematic cysteine-scanning methodologies have been used successfully to explore the molecular determinants of the pore-forming domain for numerous ion channels (e.g., Wilson and Karlin, 1998; Engh and Maduke, 2005; Li et al., 2008), but this strategy has been limited to the application of thiol probes from the external side of CFTR probably due to technical challenges imposed by the 18 endogenous cysteines present mostly in the cytoplasmic domains of CFTR. Among CFTR's 12 TMs, TM6 has been studied most extensively. However, cysteine-scanning studies of TM6 by using externally applied thiol reagents have generated conflicting results among different groups, as summarized in Alexander et al. (2009).

Recent construction and successful functional expression of a CFTR construct with all endogenous cysteines substituted (cysless) have made it possible for cross-linking (Cui et al., 2006; Mense et al., 2006) and cysteine-scanning experiments (Alexander et al., 2009; Zhou et al., 2010). In the present study, we chose TM6 (residues 330–335) as our first candidate for cysteine-scanning experiments because nearly all previous work has implicated this segment as one of the pore-forming domains (for reviews see McCarty, 2000; Dawson et al., 2003; Linsdell, 2006). For example, the positively charged amino acids R334 and K335 have been shown to serve as potential surface charges to promote entry of anions into the outer mouth of the pore (Smith et al., 2001). Evidence has also been gathered that T338, located one helical turn cytoplasmic to R334 and K335, may face the pore as a cysteine residue placed at this position can not only be modified by methanethiosulfonate (MTS) reagents, but also titrated with external protons (Liu et al., 2004). This same position has been implicated by several studies using various strategies as the narrow part of the pore as viewed from the extracellular end of the pore (Linsdell et al., 2000; McCarty and Zhang, 2001; Alexander et al., 2009). Although mutations of several residues in TM6 intracellular to T338 do affect anion conductance and the affinity for CFTR blockers (for review see Linsdell, 2006), detailed understanding of the cytoplasmic half of TM6 beyond position 338 is limited.

Here, we engineered cysteine one at a time into TM6, applied, from the cytoplasmic side of the channel, positively charged 2-trimethylammonium-ethyl MTS (MTSET) and negatively charged 2-sulfonato-ethyl MTS (MTSES), and monitored in real time the current response to these reagents in excised inside-out membrane patches. We found that both MTSET and MTSES can react with the cysteines introduced at six positions (S341, I344, V345, M348, R352, and Q353). The reactivity pattern is consistent with the idea that TM6 can be divided into internal and external parts connected by a constricted region close to S341. Our data also support the notion that the internal part of TM6 (S341 to Q353) assumes a secondary structure of an α helix, and the reactive sites reside in two adjacent faces of the helix.

Interestingly, although the negatively charged MTSES inhibits currents generated by these mutants through reducing the single-channel amplitude, the positively charged MTSET poses only slight influence on the single-channel amplitude in most cases, except at position 352, where the R-to-C mutation decreases the single-channel amplitude; however, bringing back the positive charge with MTSET or 2-amino-ethyl MTS (MTSEA) restores the conductance. Surprisingly, effects on both the open time and the closed time are found when positively charged MTS reagents are deposited into each of the three positions (344, 348, and 352) that line one face of the helix. These results suggest that these positions are involved in the gating conformations changes. By measuring the modification rate and its dependence on the membrane potential, we were able to deduce that residues 341, 344, and 345 are located deep in the membrane field and/or in the narrow region of the pore, whereas residues 348, 352, and 353 are positioned in the wide cytoplasmic end of the helix.

MATERIALS AND METHODS

Mutagenesis, cell culture, and transient expression

An original cysless CFTR construct was provided by B. Reenstra (University of Pennsylvania, Philadelphia, PA). In this construct, 16 cysteines were mutated to serines, and two cysteines (C590 and C592) to leucines. Subsequently, an additional V510A mutation was introduced to promote expression (Wang et al., 2007). A single cysteine was then engineered into each position in TM6 on the cysless/V510A background using the QuikChange XL kit (Agilent Technologies). Mutations were confirmed by direct DNA sequencing (DNA core; University of Missouri) of the cDNA. Because all of our studies were performed under this cysless/V510A background, we will refer to this construct as our wild-type (WT) cysless control.

The Chinese hamster ovary cells were grown at 37°C in Dulbecco's modified Eagle's medium supplemented with 10% fetal bovine serum. The cDNA constructs of CFTR were cotransfected with pEGFP-C3 (Takara Bio Inc.) encoding green fluorescent protein, using PolyFect transfection reagent (QIAGEN) according to the manufacturer's protocols. The transfected cells were plated on sterile glass chips in 35-mm tissue culture dishes and incubated at 27°C for 2–5 d before electrophysiological experiments were performed.

Electrophysiology

Membrane currents were recorded in inside-out patch clamp configuration at room temperature (22–24°C). Borosilicate capillary glass was pulled with a two-stage vertical puller (Narishige) and subsequently fire-polished with a homemade microforge, yielding a pipette resistance of 2–5 MΩ when filled with the pipette solution (in mM: 140 NMDG-Cl, 2 $MgCl_2$, 5 $CaCl_2$, and 10 HEPES, adjusted to pH 7.4 with NMDG). Glass chips with transfected cells grown on were placed into a chamber on the stage of an inverted microscope (Olympus). The chamber was continuously perfused, initially with the bath solution (in mM: 145 NaCl, 5 KCl, 2 $MgCl_2$,

1 $CaCl_2$, 5 glucose, 5 HEPES, and 20 sucrose, adjusted to pH 7.4 with NaOH), and later on with the standard perfusate (in mM: 150 NMDG-Cl, 10 EGTA, 10 HEPES, 8 Tris, and 2 $MgCl_2$, adjusted to pH 7.4 with NMDG). Patches with seal resistances of >40 GΩ were excised for further experiments. Current signals at −50 mV membrane potential (unless specified otherwise) were acquired with a patch clamp amplifier (EPC10; HEKA), filtered at 100 Hz with an eight-pole Bessel filter (Warner Instruments), digitized online at 500 Hz with Pulse software (V8.80; HEKA), and captured onto a hard disk. Fast solution exchange was achieved using a solution exchange system (SF-77B; Warner Instruments), which can minimize the delay in the solution exchange to ∼30 ms as determined previously (Tsai et al., 2009).

Cysteine modification

MTS reagents (MTSES, MTSET, and MTSEA; Toronto Research Chemicals Inc.) were prepared as 100-mM stock solutions in ddH_2O stored at −70°C. Immediately before use, a single aliquot of the stock solution was thawed into the perfusion solution containing 2 mM ATP. In most cases (Figs. 1 and 3–10), 1 mM of the MTS reagents was used, but the MTSES concentration was lowered to 50 µM (Fig. 11) for cysteine-substituted mutants with fast modification rates.

Two technical precautions were taken to ensure the quality of our data. First, spontaneous oxidation of the thiol group has been reported to protect the engineered cysteine from MTS modification (Li et al., 2005; Liu et al., 2006). In theory, this reaction could happen during the activation phase of our experiments, as phosphorylation of the channels by PKA usually takes 3–10 min to reach a steady state. We therefore added 10 mM dithiothreitol (DTT; Sigma-Aldrich) into the solution containing PKA to ensure that the introduced cysteine is mostly in a reduced form. Second, because the presence of membrane-associated protein phosphatases in excised patches (e.g., Luo et al., 1998; Zhu et al., 1999) could give rise to false positive hits when a decrease of the current is used as a marker, all MTS reagents were added after a stationary recording was established with ATP alone. An absence of current decrease with ATP alone ensures that the observed reduction of the current upon the addition of the MTS reagent is indeed caused by modification of the introduced cysteine.

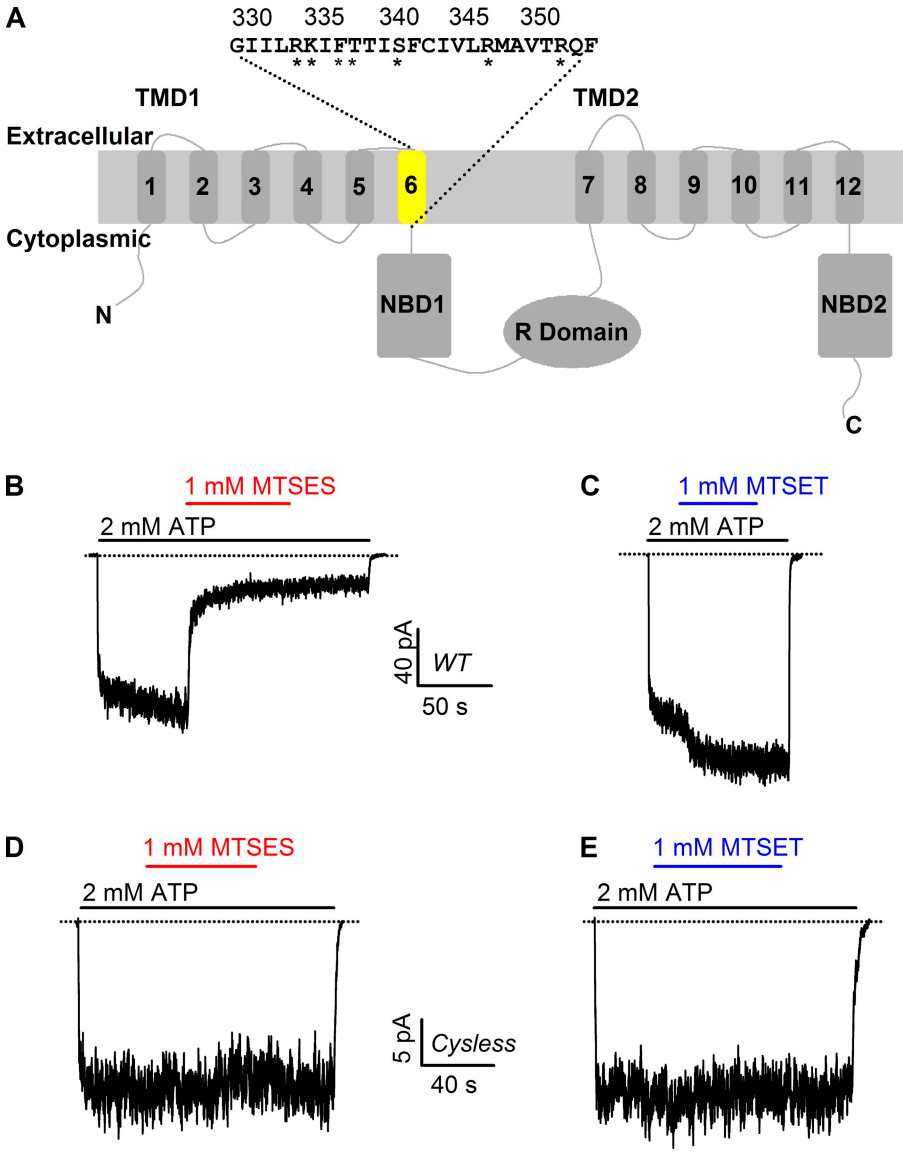

Figure 1. Cysless CFTR is an appropriate background for cysteine scanning. (A) Topological diagram of CFTR showing its domain architecture: two TMDs, two NBDs, and one R domain. Each TMD contains six TMs (1–6 and 7–12) connected by intracellular and extracellular loops. Cysteines were introduced into TM6 (yellow). The sequence of TM6 is shown, and residues where cysteine-substitution affects single-channel amplitude are indicated by stars. (B and C) Modification of phosphorylated WT CFTR channels by MTSET and MTSES. After the ATP-induced current reached a plateau, the solution was exchanged from ATP to ATP plus MTSES or MTSET using the fast solution exchange system (see Materials and methods). The solution was switched back to ATP after the MTS reagents took full effect. The dotted line represents the baseline in all figures. (D and E) Similar protocols as in B and C showing that cysless CFTR channels do not respond to the treatment of MTS.

Data analysis

Current traces containing fewer than three channel opening levels and lasting for >1 min were selected for single-channel kinetic analysis using a program developed by L. Csanády (2000). A three-state kinetic model, C↔O↔B, was adopted to extract gating parameters (open time, closed time, and Po) as described previously (Bompadre et al., 2005). Single-channel amplitude was estimated by Gaussian fitting of the all-point amplitude histogram with the multi-peak fitting package in the Igor Pro program (V4.07; WaveMetrics).

For the modification of MTSES, the apparent second-order reaction rate constant was calculated as $1/(\tau \times [\text{MTSES}])$, where τ was measured by fitting the current decay phase upon the addition of MTSES with a single-exponential function.

All results were presented as means ± SEM; n represents the number of experiments. Student's paired or unpaired t test (two-tailed) was performed with Excel 2007. $P < 0.05$ was considered significant.

RESULTS

Cytoplasmically applied MTS reagents alter the channel function of WT CFTR, but not cysless CFTR

A construct that shows little response toward thiol-modifying reagents is a prerequisite for cysteine-scanning studies. However, there are 18 endogenous cysteines scattering through all five domains of the WT CFTR protein. Reactivity of one or several of these cysteines toward MTS reagents was observed when the reagents were applied to the cytoplasmic side of inside-out membrane patches containing WT CFTR channels, which were first activated to a steady state with the catalytic subunit of PKA plus 2 mM ATP. An example of the experiments was shown in Fig. 1 B. ATP-induced channel activity was decreased by fivefold during exposure to 1 mM MTSES, a negatively charged MTS reagent, and remained at the decreased level after removal of the reagents. In contrast, 1 mM MTSET, a positively charged MTS reagent, modestly increased the WT channel current (Fig. 1 C). To generate the background required for our studies, we made a cysless CFTR construct by mutating all endogenous cysteines (see Materials and methods for details). Macroscopic currents from cysless CFTR could be similarly elicited by ATP as WT channels but were insensitive to cytoplasmic-applied MTSES or MTSET (Fig. 1, D and E). Moreover, the single-channel current amplitude of cysless CFTR is only slightly altered (not depicted), similar to previous reports (Cui et al., 2006; Mense et al., 2006). Overall, these properties of this cysless (or cysless/WT) CFTR make it an appropriate background for assessing the reactivity of subsequently introduced cysteines in TMDs of CFTR with thiol-modifying reagents.

Reactivity of substituted cysteines in TM6 to MTS reagents

We introduced cysteines, one at a time, throughout TM6 (residues 330–354) on the cysless/WT construct. The effects of cysteine substitution on anion permeation can be first inferred from the change in the single-channel current amplitude. 7 out of the 25 mutant channels exhibited a reduced single-channel current amplitude, including, from extracellular to intracellular, R334C, K335C, F337C, T338C, S341C, R347C, and R352C (Fig. 2). The single-channel amplitude is unsolvable in the cases of R334C, S341C, R347C, and R352C due to a limited bandwidth, whereas it is 0.2–0.3 pA for

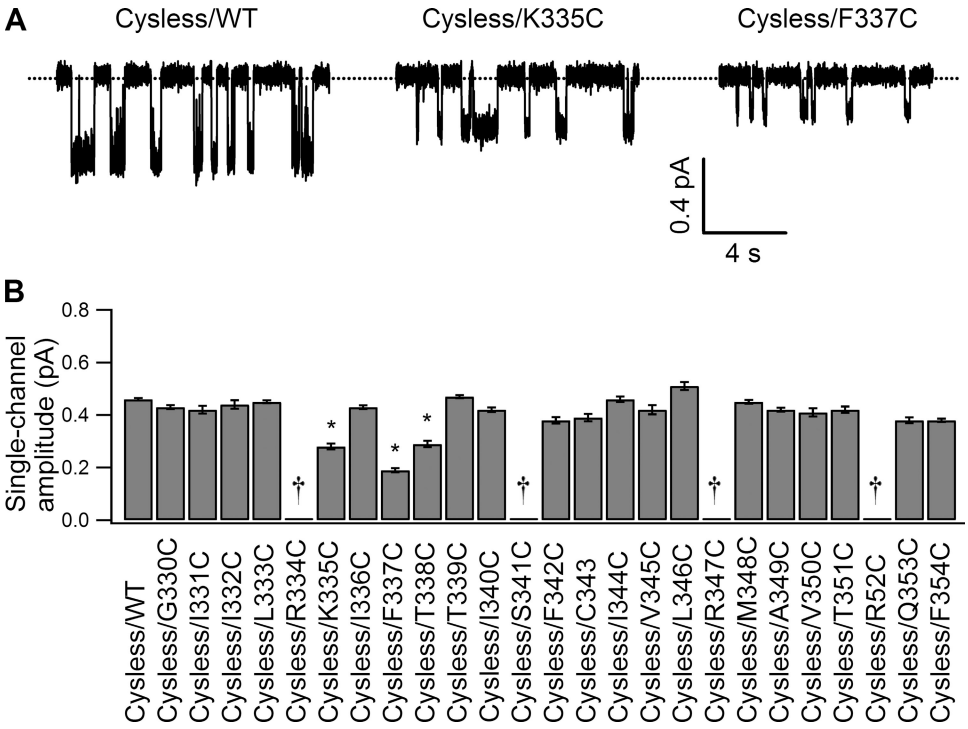

Figure 2. Effects of cysteine substitutions on single-channel current amplitude. (A) Single-channel traces for cysless/WT and two cysteine-substituted mutants. Single-channel amplitude: cysless/WT, 0.46 ± 0.005 pA (n=5); cysless/K355C, 0.28 ± 0.011 pA (n = 4); cysless/F337C, 0.19 ± 0.008 pA (n=3). (B) Summary of the single-channel amplitude for cysless/WT and all mutant channels. The data are shown as mean and SEM of three to seven experiments. Stars indicate a significant difference in the single-channel amplitude from the cysless/WT, as determined by Student's t test. Daggers indicate channels whose single-channel amplitude is too small and/or variable to be measured accurately.

K335C, F337, and T338C at −50 mV membrane potential (0.46 pA for cysless/WT). Exact structural interpretations of these effects are difficult without further characterization of the functions of these mutant channels, but it has been proposed that this alteration of the single-channel conductance could be due to neutralization of the fixed charge that serves to attract anions into the outer mouth of the pore (e.g., R334; Smith et al., 2001), disruption of a salt bridge formed between positively charged residues in TM6 and negatively charged ones in other TMs (e.g., R347; Cotten and Welsh, 1999), or removal of a potential Cl^--binding site (e.g., S341; McDonough et al., 1994).

We then studied the reactivity of each of the substituted cysteines toward intracellularly applied charged MTS reagents. After the channels were activated with PKA and ATP, 1 mM MTSES or MTSET was applied in the presence of ATP until a steady state arrived. The ATP-induced currents before and after the treatment were compared. The results of these experiments are summarized in Fig. 3. None of the cysteines engineered at positions located extracellularly to position 341 appeared to react with the reagents. Because previous studies (Smith et al., 2001; Beck et al., 2008; Alexander et al., 2009) have shown that cysteines placed at some of these positions are reactive toward the same reagents applied from the external side, it can be inferred that there is a barrier around position 341 restricting the accessibility of the bulky MTS reagents applied from the cytoplasmic side.

Cytoplasmic to position 341, the reactive cysteines can be divided into three categories based on the pattern of their reactivity toward the two reagents. Representative traces of each category are shown in Fig. 4. The first category (e.g., Fig. 4, A and B), in which negligible effects were observed with either reagent, includes cysteines introduced at positions 342, 343, 346, 347, 349, 350, 351, and 354. Although the simplest interpretation of these results is that these positions are not accessible to MTS reagents, it cannot be ruled out that they were modified but without significant effects on channel function. Cysteines falling into the second category (344, 348, and 352) were reactive toward both reagents with charge-dependent functional effects. Specifically, the macroscopic current was enhanced after the application of the positively charged MTSET, but was attenuated in response to the negatively charged MTSES (Fig. 4, C and D). Spontaneous ATP-independent gating of cysless/I344C and cysless/M348C was also increased by MTSET because after the removal of ATP, there remained a substantial amount of current, which can be inhibited by CFTR-specific inhibitor,

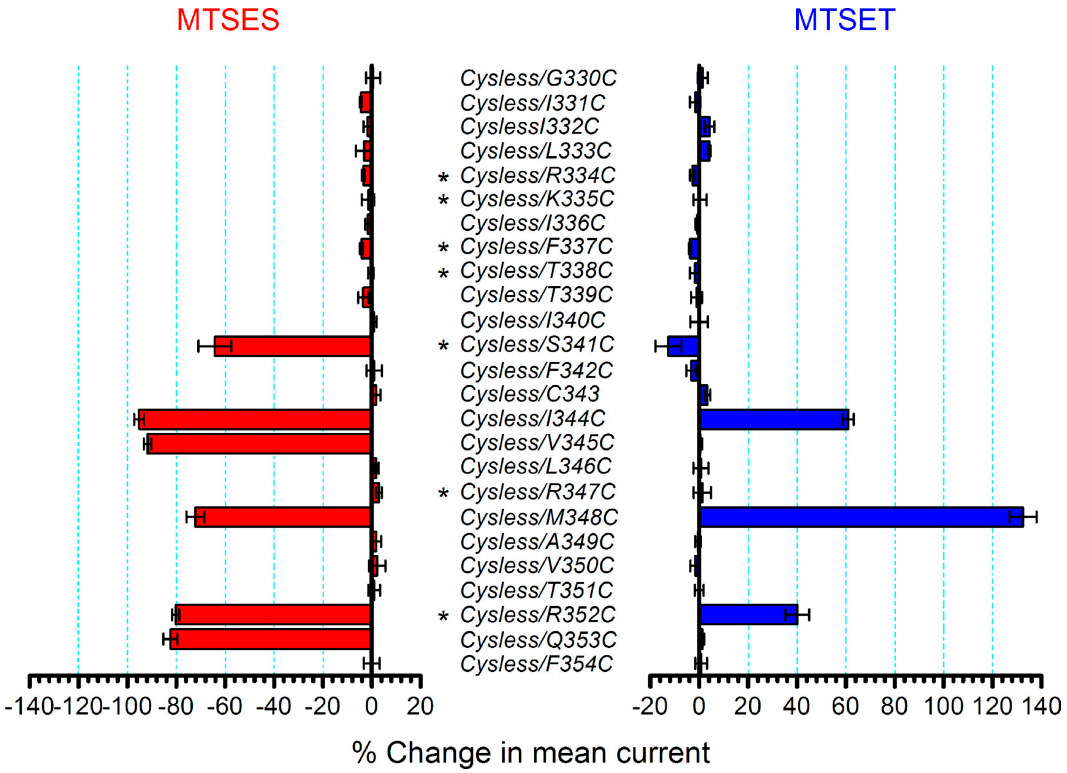

Figure 3. Summary of the change in macroscopic mean currents after modification. The percentage change in the mean current is calculated as $(I_\infty/I_0-1) \times 100\%$, where I_0 and I_∞ are the mean current before and after modification, respectively. The left column is the effect of MTSES (red), and the right is the effect of MTSET (blue). $n = 3$–8 for each construct. Stars indicate mutant channels exhibiting a reduced single-channel amplitude.

CFTRinh-172 (Ma et al., 2002). Cysteines introduced at the last three positions (341, 345, and 353) belong to the third category. Although MTSET posed small (<20% for S341C) or negligible inhibition, modification by MTSES drastically reduced the current (e.g., Fig. 4, E and F). The observation that prior MTSET modification effectively prevented the effect of MTSES indicates that cysteines 345 and 353 did react with MTSET. It is noted that cysteines in the second category (344, 348, and 352) are separated by three amino acids, and that cysteines in the third category (341, 345, and 353) follow a similar pattern, with the exception of position 349. These results are consistent with the idea that the cytoplasmic part of TM6 (from 341 to 354) assumes a secondary structure of an α helix.

Covalent modification of the cysteines substituted for M348 and I344 by positively charged MTSET increases the open probability (Po)

The charge-dependent functional effects of modification of cysteines in the second category (344, 348, and 352) are particularly intriguing because the currents were increased by MTSET modification. Although the arginine at position 352 is a charged residue and converting this R to C did change the single-channel amplitude, this is not the case for residues 344 and 348 (Fig. 2). In addition, MTSET modification can more than double the current in M348C channels. Therefore, it seems unlikely that this effect of modification is caused solely by a change of the single-channel conductance. We resorted to single-channel recordings and performed all-point histogram and gating kinetics analysis to further examine the effects of MTSET modification. A representative result of the experiments with the cysless/M348C construct is shown in Fig. 5. In the presence of ATP, the cysteine-substituted channel exhibited a similar single-channel amplitude (Fig. 2 B) but a lower open probability (Po = 0.24 ± 0.03; $n = 5$) compared with the cysless/WT channel (0.64 ± 0.02; $n = 5$; Fig. 5, A and B). Upon the application of the positively charged MTSET, channel gating behavior was profoundly altered (Fig. 5, A and B). Both the open time and opening rate were

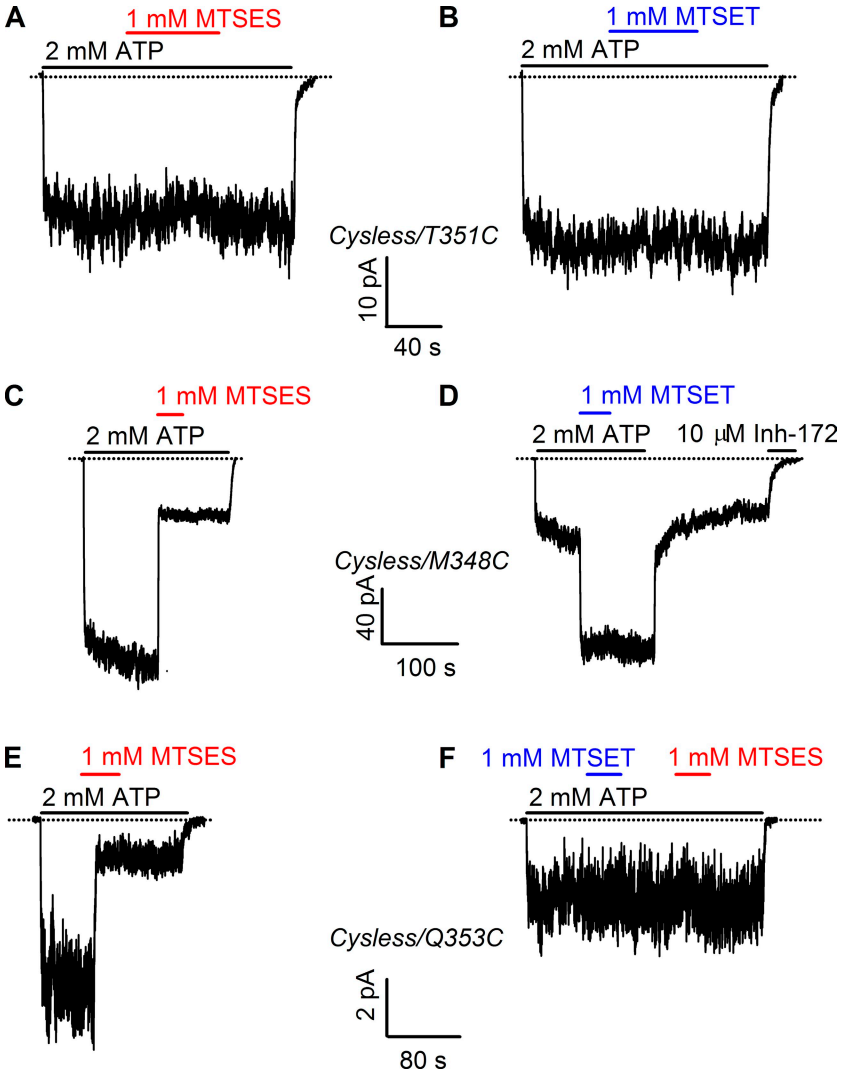

Figure 4. Three different patterns of functional consequences after MTS modification. (A and B) Neither MTSES nor MTSET altered the current of cysless/T351C channels. (C) Modification of 348C by MTSES decreased the current. (D) MTSET increased ATP-dependent current in cysless/M348C channels. After the removal of ATP, there remained a large amount of ATP-independent current, which disappeared upon the application of 10 μM CFTRinh-172. (E) MTSES reduced the current of cysless/Q353C channels. (F) For cysless/Q353C, the treatment of MTSET had little influence on channel function, but prevented the current decrease in response to MTSES, as in E.

visibly increased, resulting in a Po threefold higher than that before modification. Interestingly, MTSET modification of M348C also slightly but significantly increased (12 ± 1%; $n = 5$) the single-channel amplitude (Fig. 5, A and C). The effects on both gating behavior and anion conduction were readily reversed after the patches were exposed to 10 mM DTT, a commonly used reducing reagent (e.g., Liu et al., 2006; Reyes and Gadsby, 2006). These results indicate that the effects of cysteine substitution as well as the subsequent modification by MTSET on Po are mainly through perturbing the conformational changes around this site of TM6 associated with gating (see Discussion for more details).

Effects on channel gating were also observed with modification of the cysteine residue engineered into position 344, one helical turn extracellular to 348, as shown in Fig. 6. The mutant channel showed a similar Po (Fig. 6 B) and single-channel amplitude (Fig. 2 B) as the cysless/WT channel. However, modification by MTSET dramatically increased the open time, which was too long (on the order of tens of seconds) for collecting enough gating transitions for kinetics analysis. The Po was increased from 0.65 ± 0.02 ($n = 7$) to 0.92 ± 0.01 ($n = 7$; Fig. 6 B) after modification. A minor effect on anion conduction after MTSET modification was also observed (Fig. 6 C); that is, the single-channel amplitude was decreased by 5 ± 1% ($n = 7$). Again, gating behavior and conduction properties were recovered after the application of 10 mM DTT.

Covalent modification by positively charged MTS reagents of the cysteine substituted for R352 not only restores Cl^- conduction, but also alters channel gating

The results described above suggest that the side chains of the amino acid residues at positions 344 and 348 of TM6 are involved in the gating conformational changes. We further characterized the effects of modification of the cysteine substituted for the positively charged arginine residue at the more cytoplasmic position 352, as this position is one helical turn intracellularly to position 348. Some previous studies have suggested that this residue may serve to attract anions into the intracellular pore mouth via a "surface charge" effect (Aubin and Linsdell, 2006). Others provide evidence that it might form a salt bridge with residue D993 in TM9, and that neutralizing the positive charge at this position indirectly affects anion conduction (Cui et al., 2008; Jordan et al., 2008). It has also been reported that charge-neutralizing mutation at this position would lead to frequent transitions to subconductance states and rare transitions to full-conductance states (Cui et al., 2008). Fig. 7 depicts a representative recording of a patch containing a single cysless/R352C CFTR channel. In the presence of ATP, the mutant channel opens to small

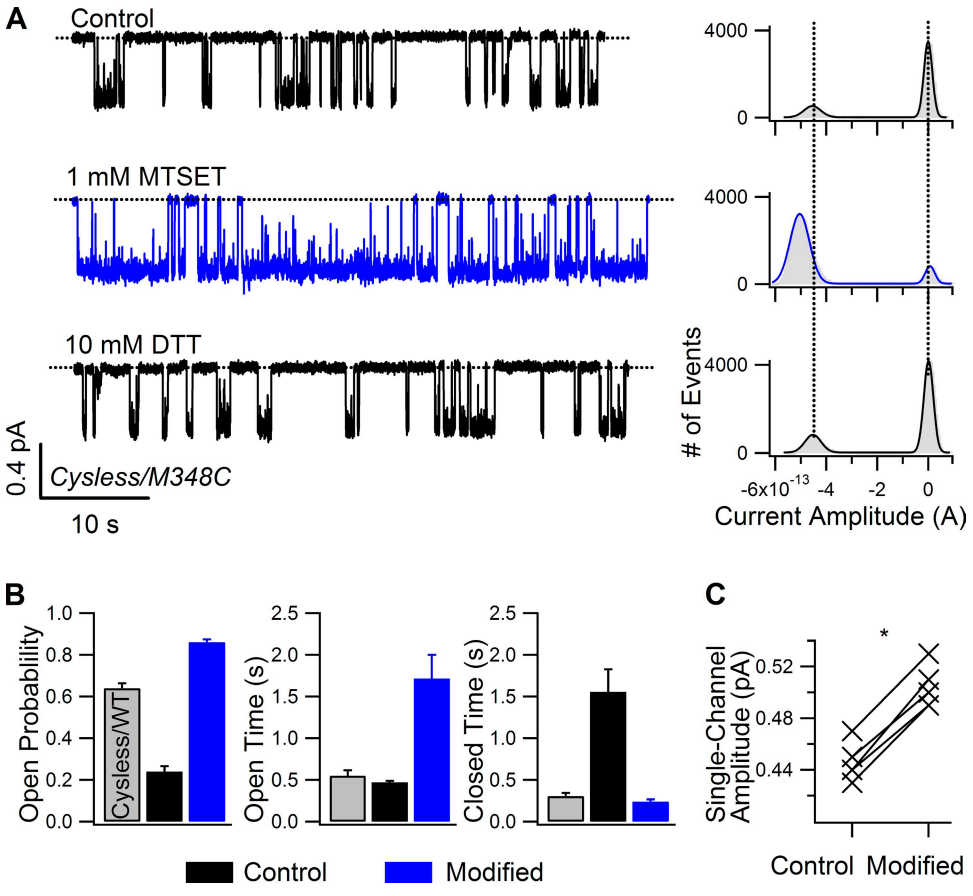

Figure 5. Effects of MTSET on a single cysless/M348C channel. (A) Single-channel traces in the presence of 2 mM ATP before (left top trace) and after MTSET modification (left middle trace, blue), and after DTT treatment (left bottom trace) in the same patch. Corresponding all-point histograms (gray bars) and their Gaussian fits (black and blue lines) were plot on the right. (B) Gating parameters of the cysless/M348C channel before (black) and after (blue) modification, as extracted from the traces in A. Those of the cysless/WT (gray) in the presence of 2 mM ATP are also included for comparison (traces not depicted). $n = 5$ for cysless/M348C. $n = 6$ for cysless/WT. (C) Single-channel amplitude of the cysless/M348C channel before and after modification in the same patch. Star indicates significant difference as determined by Student's paired t test; $n = 5$.

and unsynchronized current levels (0.1–0.2 pA), different from the fairly constant amplitude observed in the cysless/WT channel. But no full-conductance state was ever observed during minutes of recording, probably due to the limited bandwidth of our recording condition. The gating kinetics cannot be accurately determined because of the small and varying single-channel amplitude. However, when R352C was modified by MTSET, the single-channel amplitude was restored to that of the cysless/WT channel (Fig. 7 A). This effect of MTSET on the single-channel amplitude allows kinetic analysis of the modified channels (Fig. 7 B). Interestingly, although bringing back the positive charge at this position with MTSET completely restores the single-channel amplitude, gating of MTSET-modified cysless/R352C is not fully recovered to the level of cysless/WT channels. The open time (0.29 ± 0.01 s; n = 5) was shorter, and the closed time (1.9 ± 0.04 s; n = 5) was longer. In the same patch, after the MTSET adduct was removed by DTT, MTSEA, another positively charged MTS reagent with an amine group different from that of MTSET, also restored the single-channel amplitude. However, the gating behavior was different from that of channels modified by MTSET. The open time was significantly prolonged (0.49 ± 0.05 s; n = 7), and the closed time was also shortened considerably (0.86 ± 0.12 s; n = 7), resulting in a Po of MTSEA-modified channel nearly three times that of MTSET-modified channel. The nearly identical effect on the single-channel amplitude but a distinct influence on gating by MTSET and MTSEA suggests that the arginine residue at position 352 plays two roles: first, the positive charge it bears does affect anion permeation through the CFTR pore, and second, just like residues 344 and 348, this part of TM6 is likely involved in gating motion (see Discussion for details).

The restoration of the single-channel amplitude by MTSET or MTSEA on R352C compelled us to use another strategy to assess the function of the CFTR pore before and after modification. Fig. 8 shows results obtained from patches yielding macroscopic cysless/R352C channel currents. The modification by MTSET increased the mean current by 40 ± 4.9% (n = 4; Fig. 8, A and C), whereas modification by MTSEA increased it by 293 ± 28.5% (n = 6; Fig. 8, B and C). Because these two MTS reagents restored the single-channel amplitude to the same level, the distinct effects on the macroscopic mean current was due to their different effects on channel gating. To study the effects of modification on the pore structure, we applied an anionic pore blocker, glibenclamide (Sheppard and Robinson 1997; Zhou et al., 2002), before and after modification with MTSET or MTSEA. When the membrane voltage was held at −50 mV, 50 μM glibenclamide induced 27.2 ± 1.7% (n = 10) block of the Cl^- current for cysless/R352C. Because the same concentration of

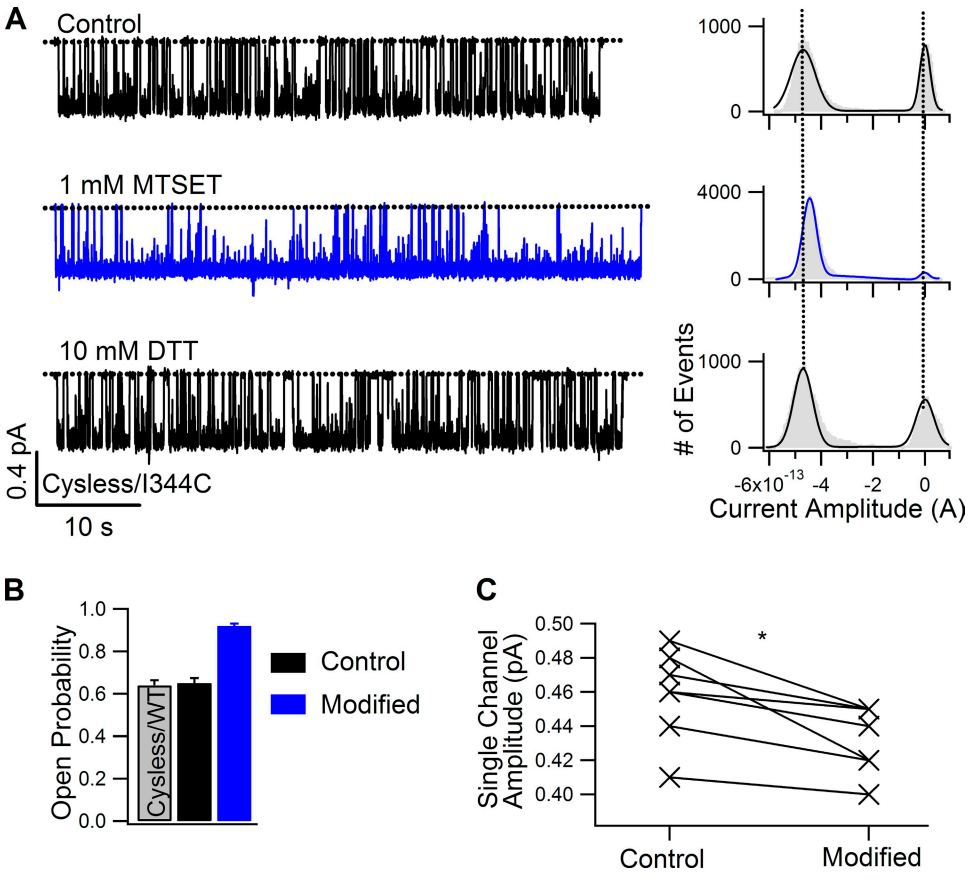

Figure 6. A single-channel recording of cysless/344C showing the effect of MTSET. (A) Gating behavior in the presence of 2 mM ATP before modification (left top trace), after modification (left middle trace, blue), and after the reversal of the modification by DTT (left bottom trace) in the same patch. Corresponding all-point histograms (gray bars) and their Gaussian fits (black and blue lines) were plot on the right. (B) The Po, obtained from the traces in A, of the cysless/I344C channel before (black) and after (blue) modification. Those of the cysless/WT (gray) in the presence of 2 mM ATP are included for comparison (traces not depicted). n = 7 for cysless/I344C. n = 6 for cysless/WT. (C) Single-channel amplitude of the cysless/I344C channel before and after modification. Star indicates significant difference as determined by Student's paired t test; n = 7.

glibenclamide at the same holding potential induced stronger block in the cysless/WT channel (48.6 ± 3.0%; $n = 5$; Fig. 8 D), the effect of the blocker was attenuated by the R352C mutation. Bringing back the positive charge through modification by MTSET increased the fractional block to 44.1 ± 1.9% ($n = 7$; Fig. 8, A and D). Similarly, the modification by MTSEA increased it to 47.0 ± 1.6% ($n = 6$; Fig. 8, B and D). Thus, the blockade of the CFTR channel pore by glibenclamide relies in part on the positive charge at position 352. Collectively, we conclude that restoring the positive charge at this position confers a normal function of the pore in the context of chloride permeation and blockade of the pore by glibenclamide. However, the effect of charge-restoring modifications on gating depends on the specific chemical properties of the MTS reagents.

Covalent modification by negatively charged MTSES decreases Cl^- conduction

Although, as described above, modifications of 344C, 348C, and 352C with positively charged MTS reagents can alter gating, it is unclear if the decrease of macroscopic current by MTSES for 341C, 344C, 345C, 348C, 352C, and 353C was due to an effect on channel gating or anion permeation. Because anion conduction was severely perturbed by the mutations R352C and S341C, we were not able to assess the effects of MTSES modification on the single-channel amplitude for these two constructs. Instead, we will focus on the four other positive hits (i.e., I344C, V345C, M348C, and Q353C). Fig. 9 depicts a sample experiment with the cysless/Q353C construct. After the channel was treated with MTSES, the single-channel amplitude was visibly decreased but cannot be quantified due to a large variation of the single-channel current amplitude. The negatively charged adducts were hardly removable by the anionic DTT (not depicted), probably due to unfavorable electrostatics between MTSES adduct and negatively charged reactive DTT as described by Alexander et al. (2009). For the positions 344, 345, and 348, however, single-channel recordings are not helpful because no visible current

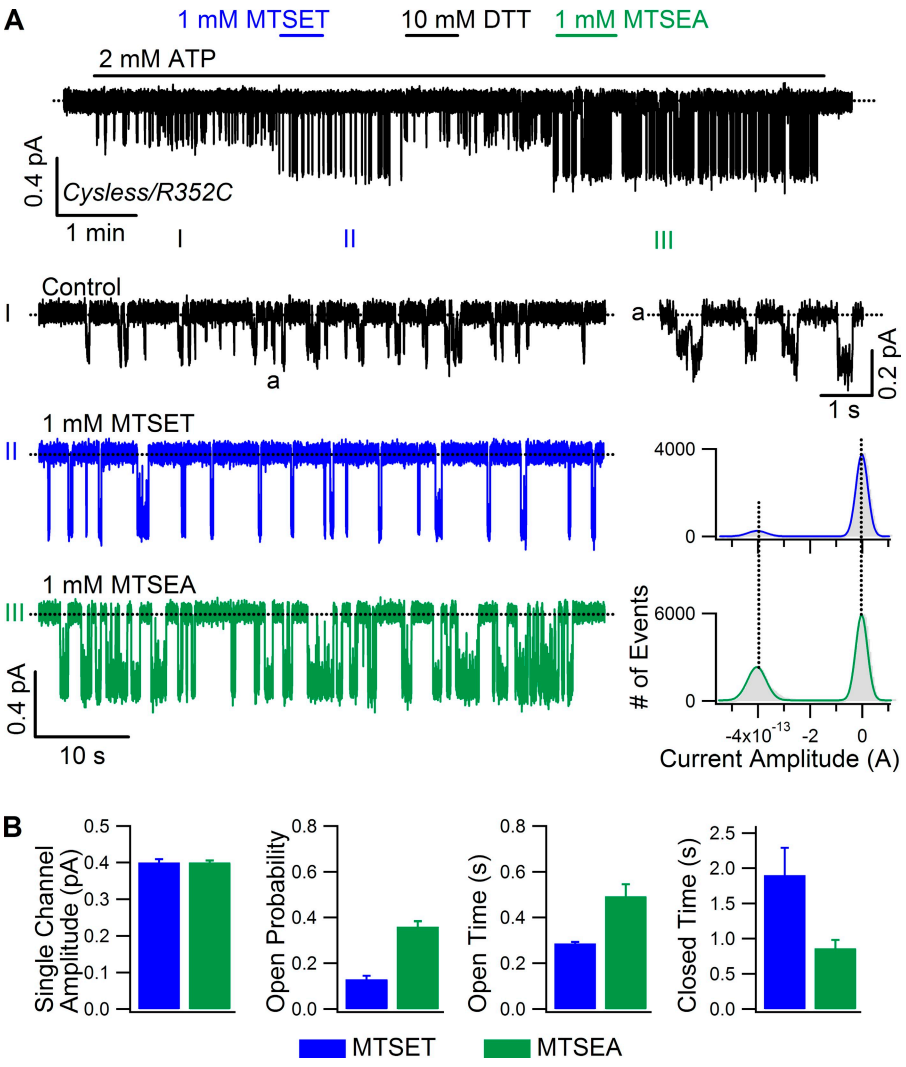

Figure 7. A single-channel recording showing that modification of 352C by MTSET and MTSEA affects both Po and single-channel amplitude. (A; top trace) A continuous recording showing the effects of MTSET or MTSEA on a single cysless/R352C channel. (Bottom traces) Expanded recordings for segments I–III marked in the top trace. A short part in segment I was further zoomed out in a. Corresponding all-points amplitude histograms of II and III were depicted. Blue and green lines are the results of Gaussian fitting. (B) Single-channel amplitude, Po, open time and closed time of MTSET- (blue) and MTSEA-modified (green) cysless/R352C channel, as determined by Gaussian fitting and kinetics analysis; $n = 6$.

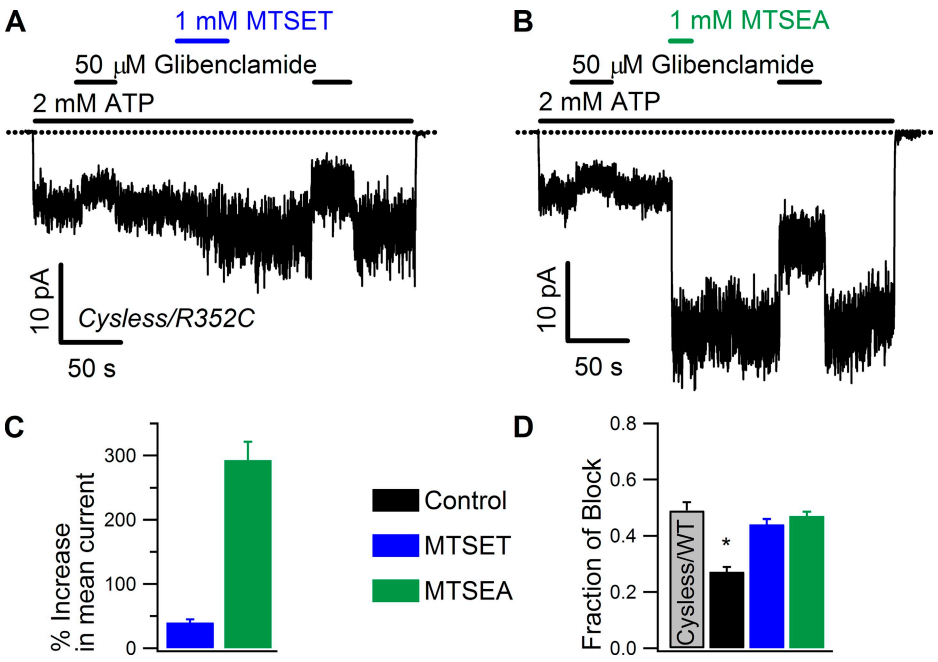

Figure 8. Blocking of cysless/R352C channels by glibenclamide before and after MTS modification. (A and B) The blocking effect of 50 µM glibenclamide was enhanced after the channels were modified by MTSET and MTSEA. (C) Percentage change in mean current induced by MTSET (blue) and MTSEA (green). (D) The fraction of block, calculated as $(1-I_g/I_0) \times 100\%$ (I_g and I_0 are the mean current in the presence of ATP and ATP plus glibenclamide, respectively), for cysless/WT channels (gray), cysless/R352C channels before modification (black) and after modification with MTSET (blue), and after modification with MTSEA (green). Star indicates a significant difference from cysless/WT channels.

fluctuation was seen after modification in patches yielding microscopic currents (not depicted). This could be due to either an extremely small single-channel amplitude or minimal opening probability. In a representative recording of a patch containing hundreds of cysless/I344C channels (Fig. 10), one can clearly discern the single-channel amplitude from the expanded trace before and after phosphorylation-dependent activation. Before MTSES modification, these single-channel amplitudes are similar to that of the cysless/WT channel (Fig. 2). After MTSES modification, a dramatic reduction of the macroscopic current occurred. Upon removal of ATP, a very smooth current relaxation reflecting the closing of individual MTSES-modified channels was seen (Fig. 10, red expanded trace), indicating that the single channel-amplitude of MTSES-modified channels was too small to be resolved. Similar results were obtained with the cysless/V345C and cysless/M348C channels. Thus, depositing negative charges at these three positions (344, 345, and 348) severely reduces anion conduction. Although the exact reason is unknown, the discrepancy between the extent of inhibition of the macroscopic mean current (Fig. 4 C) and the single-channel current in the case of the cysless/M348C channel might be due to oxidation of the introduced cysteine to a state not reactive toward either DTT or MTS reagents. Similar oxidized states of cysteine thiolates engineered at position 338 that are not reversed by DTT were previously reported by Liu et al. (2006). Moreover, whether MTSES also affects gating is unknown because the small single-channel amplitude after modification precludes gating kinetics analysis.

Effects of membrane potential on the rate of MTSES modification

While inspecting the current changes upon the addition of MTSES, we noticed dramatic differences in the rate of current decay among different constructs. To further quantify the accessibility of engineered cysteines to the intracellularly applied MTS reagents, we measured the modification rates of MTSES for engineered cysteines at six positions with large functional effects. At a membrane potential of −50 mV, MTSES modified introduced cysteines at the more superficial

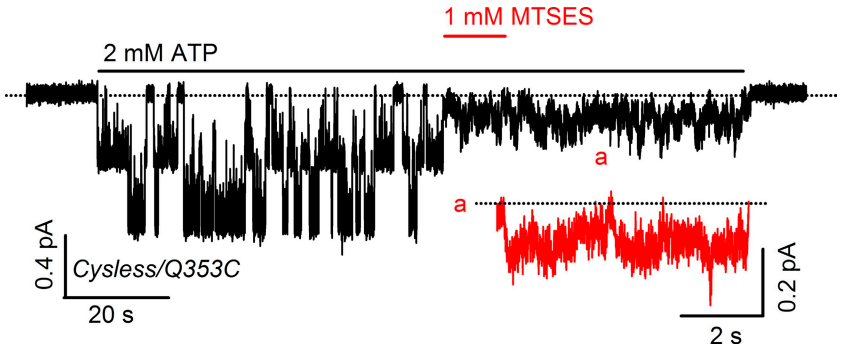

Figure 9. Modification of 353C by negatively charged MTSES reduced the single-channel amplitude. This representative recording (among five patches) contains two cysless/Q353C channels. After the application of MTSES, the single-channel amplitude was reduced. Segment a (red) is expanded to show the varying single-channel amplitude after modification.

positions 348 (9,076 ± 983 $M^{-1}s^{-1}$; $n = 5$) and 353 (2,715 ± 646 $M^{-1}s^{-1}$; $n = 4$) rapidly (Fig. 11). However, although 352C is also physically close to the cytoplasmic end, its modification rate is >100 times slower than that of 348C. The reason for this slow reaction rate is unclear, but it could be due to a perturbation of the pore architecture by the R352C mutation (Cui et al., 2008). For deeper positions, cysteine modification is rather slow: second-order reaction rate constants are 596 ± 73 $M^{-1}s^{-1}$ ($n = 7$), 20 ± 0.6 $M^{-1}s^{-1}$ ($n = 3$), and 6 ± 0.8 $M^{-1}s^{-1}$ ($n = 5$) for 344C, 345C, and 341C, respectively. Compared with the rate constant for MTSES reaction with free mercaptoethanol (17,000 $M^{-1}s^{-1}$; Karlin and Akabas, 1998), these slow modification rates suggest that these positions (341, 344, 345, and 352) in TM6 are not readily accessible to the MTS reagents. In other words, the accessibility of the MTS reagents might be restricted by physical or chemical barriers around these positions.

We reasoned that if the residue is located deep in the electric field and MTSES has to traverse significantly into the field to react with the engineered cysteine, the modification rate can be enhanced by hyperpolarizing the membrane potential. A representative experimental result with the cysless/V345C construct is shown in Fig. 11 A. The modification rate by 1 mM MTSES when the membrane voltage was held at −100 mV was five times faster than that when it was at −50 mV. And it was even more rapid when the membrane potential was hyperpolarized to −150 mV (Fig. 11 C). Similar voltage-dependent reaction rates were observed for modification of 341C and 344C. The reaction rate was 10-fold faster at −150 mV than that at −50 mV. In contrast, the modification rates by 50 µM MTSES at −50 and −100 mV were not significantly different for 348C (Fig. 11 B). Similarly, the membrane potential had negligible effects on the modification rate for 352C and 353C. These data suggest that residues cytoplasmic to M348 do not reside in the electrical field. The structural implications of these results will be discussed.

DISCUSSION

Our cysteine-scanning study on TM6 under a cysless CFTR background reveals that this TM governs both gating and permeation properties of the channel pore. The reactivity of engineered cysteines to intracellularly applied probes suggests that part of TM6 (residues 341–354) is exposed to the cytoplasm and assumes an α-helical structure. Surprisingly, cysteine modification by positively charged probes had minimal influence

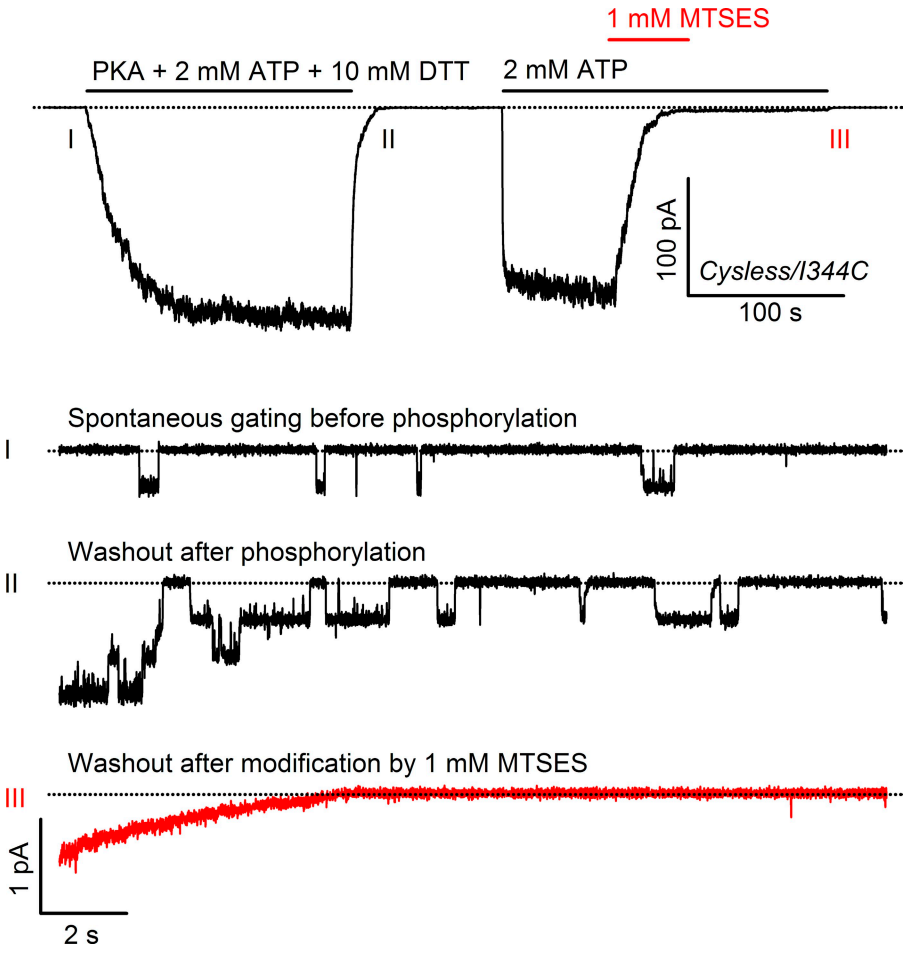

Figure 10. MTSES decreased single-channel amplitude of cysless/I344C channels. (Top trace) A continuous recoding from a patch containing hundreds of channels first phosphorylated with PKA, ATP, and DTT (see Materials and methods) until the current is steady. The current in the presence of ATP was dramatically reduced by the treatment of MTSES. (Bottom traces) Expansions of segments I–III marked in the top trace. Segment I shows spontaneous openings in the absence of ATP. Segments II and III show the current relaxation after the removal of ATP.

on anion permeation in most cases, but dramatically affected the gating behavior for three positions that line on one face of the helix. In contrast, the modification by negatively charged reagents strongly inhibited anion permeation.

Accessibility pattern and its implications on the secondary structure of TM6

Previous cysteine-scanning studies using externally applied probes (Beck et al., 2008; Alexander et al., 2009) suggest that T338 is the innermost position accessible to impermeant MTS reagents (compare Fatehi and Linsdell, 2008). Here, our results suggest that S341 is the outermost position that can be assessed by internal MTS reagents. Collectively, these findings are consistent with the idea that TM6 has a constriction around this region between T338 and S341 (Linsdell et al., 2000; McCarty and Zhang, 2001), which divides TM6 into intracellular and extracellular parts. Six positive hits (I331, L333, R334, K335, I336, and T338) were identified by external MTS reagents (Beck et al., 2008; Alexander et al., 2009; but cf. Fatehi and Linsdell, 2008). It is difficult to explain this pattern of reactivity with a simple helix facing the pore, as cysteines introduced into four contiguous positions react with bulky MTS reagents. Thus, either the external part of TM6 is not helical or is loosely packed so that all of these positions can be exposed to the aqueous environment, although it cannot be ruled out that this part might be involved in a very large movement during the gating process so that these positions were modified in different functional states. In contrast, the cytoplasmic-reactive

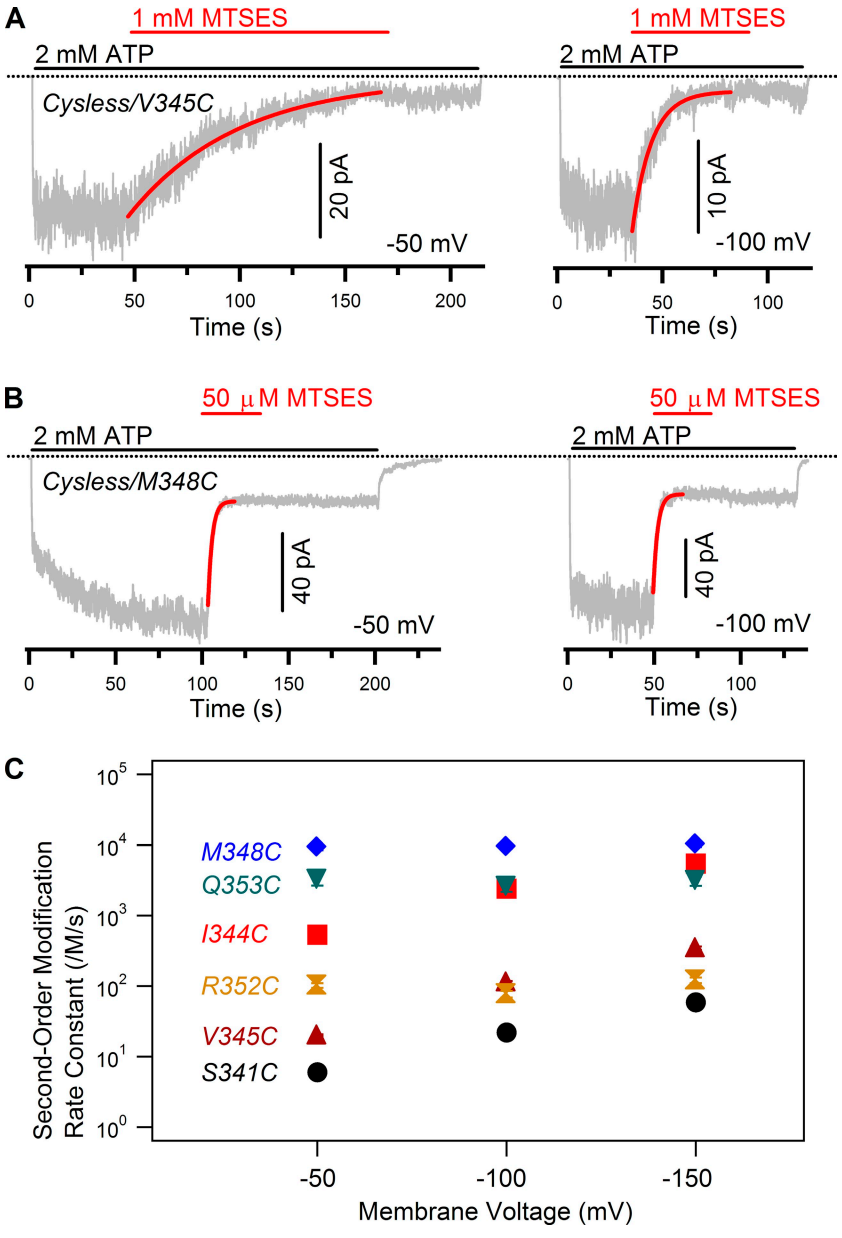

Figure 11. Reaction rates of MTSES modification at various membrane potentials. (A and B) Macroscopic recordings of cysless/V345C and cysless/M348C showing modification by 1 mM MTSES when the membrane potential is held at −50 mV (left) and −100 mV (right). Red lines are the results of exponential fitting. Note that the time scales of the left and the right traces are the same. (C) Summary of the second-order reaction rate constants at three different membrane potentials. $n = 4–7$ for each data point.

sites, S341, I344, V345, M348, R352, and Q353 (Fig. 3), can be nicely placed in two faces of a well-packed α helix if the insensitive position A349 is also included (Fig. 12 A). Interestingly, Alexander et al. (2009) applied $[Ag(CN)_2]^-$, a permeant thiol reagent, from the extracellular side and obtained similar results on most positions as ours, with the exception of F342 and A349. We do not know the reason for this discrepancy, but the much smaller size of $[Ag(CN)_2]^-$ may allow access to regions that are too narrow for bulky MTS reagents. The same reason might as well explain why A349 is the singular insensitive site on these two faces in the present study.

TM6 moves during gating transitions

Perhaps the most intriguing finding in our studies is that modification by positively charged MTSET of cysteines on one face of the TM6 helix affects channel gating (Figs. 5, 6, and 7). For both 344C and 348C, MTSET adducts increased the open time, suggesting that the open state is stabilized. The closed time is also shortened as a result of modification for 348C, indicating that the closed state is destabilized. In the case of 352C, MTSET-modified channels and MTSEA-modified channels exhibit distinct open time and closed time, which again suggests that the stability of both the open state and the closed state is different for channels with different

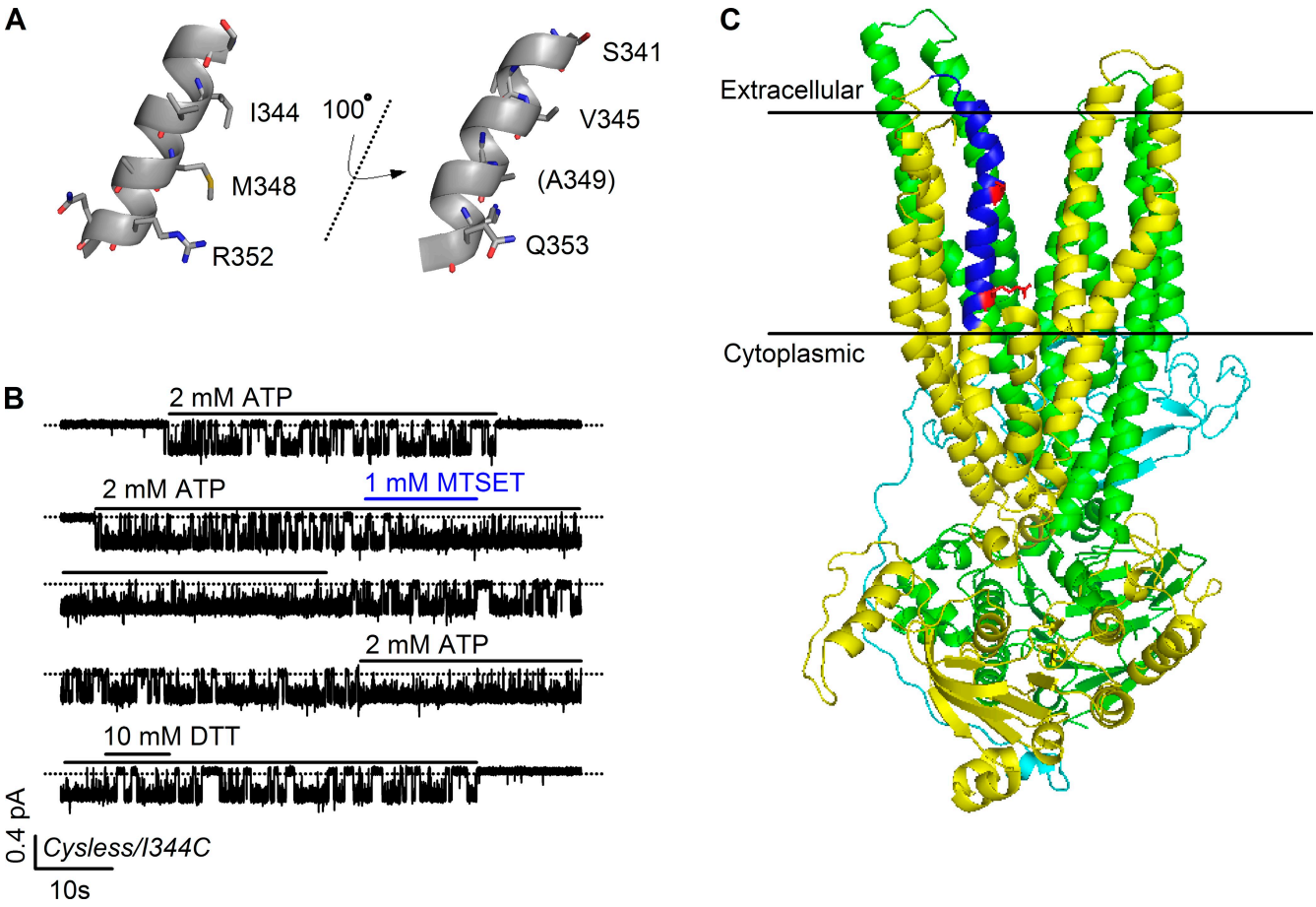

Figure 12. (A) Cartoons showing putative helical structures of part of TM6 (341–354). Structure of the cytoplasmic part of TM6 was published by Serohijos et al. (2008). Six reactive sites identified by this study were represented as colored sticks. Position 349, albeit not reactive (indicated by parentheses), was included for clarity. Figures were prepared with PyMOL (V0.99; Schrödinger). (B) A continuous single-channel recording of cysless/I344C showing a dramatic increase of the spontaneous ATP-independent gating after MTSET modification. Before MTSET modification, negligible opening events were observed in the absence of ATP. After MTSET modification, the channel activity without ATP is nearly the same as unmodified channel in the presence of ATP. This phenotype can be reversed by DTT. For spontaneous ATP-independent openings, the mean open time is 0.38 ± 0.02 s ($n = 3$) before modification (because these openings are rare, we collected events in patches yielding macroscopic currents after ATP was removed as shown in Fig. 10 and performed statistical analysis) and 0.72 ± 0.06 s ($n = 5$) after modification. Similar results were obtained for cysless/M348C: 0.36 ± 0.03 s ($n = 3$) before and 0.55 ± 0.03 s ($n = 3$) after modification. (C) Homology model of CFTR using the structure of Sav1866 as a template (adopted from Serohijos et al., 2008). The coordinate of the homology model was published by Serohijos et al. (2008). Two horizontal lines depict the possible boundaries of the membrane. TMD1 and NBD1 were colored yellow, TMD2 and NBD2 were colored green, and the R domain was colored cyan. Part of TM3 (residues 199–217) was removed to show a clear view of TM6 (residues 330–352, blue). S341 and R352 (red) were represented as sticks.

adducts. These results imply that this face of helix moves during the gating cycle.

Previous work has suggested that CFTR gating involves the movement of residues at the external part of TM6 (Zhang et al., 2005; Beck et al., 2008; Fatehi and Linsdell, 2008). However, that conclusion is mostly inferred from state-dependent accessibility of introduced cysteines. Some explored this issue by manipulating the NBDs (Zhang et al., 2005; Beck et al., 2008), and others by comparing the pre- and post-phosphorylation states (Fatehi and Linsdell, 2008). These studies, however, do not provide insights into the exact motion of TM6 during the gating cycle. In fact, the change in accessibility does not necessarily indicate a movement of the region with engineered cysteines. For example, in *Shaker* potassium channel, it has been shown that state-dependent accessibility of several introduced cysteines is caused by gating motion in regions different from the location with the introduced cysteines, which may remain relatively static during the gating conformational changes (Liu et al., 1997). Here, based on the change in the open time and the closed time between unmodified and modified channels, we propose that part of TM6 (residues 344–352) is directly involved in the gating motion of CFTR. It should be noted that only the relative motion of TM6 to other parts of the CFTR protein can be inferred here.

Gating conformational changes in the TMDs are likely driven by the dimer formation of the NBDs upon ATP binding and subsequent partial separation of the NBD dimer induced by ATP hydrolysis (Vergani et al., 2005; Zhou et al., 2006; Tsai et al., 2009, 2010). And recent statistical analysis of gating kinetics has shown that the gating cycle of the pore is tightly coupled to the ATP catalytic cycle in WT CFTR (Csanády et al., 2010). However, our results showing drastic alterations in gating kinetics caused by modulating TM6 in the TMDs (e.g., a long-lasting opening on the order of tens of seconds with the MTSET-modified cysless/I344C channel) raise the possibility that gating motion in the TMDs can also affect ATP binding and hydrolysis in the NBDs (compare Kogan et al. 2001), a subject worth more extensive future explorations.

If the MTSET adducts deposited at positions 344 and 348 indeed stabilize the open state and destabilize the closed state, one would predict that even in the absence of ATP, there will be more opening events after MTSET modification. In fact, our data show that the Po of spontaneous gating in the absence of ATP (Bompadre et al., 2007; Wang et al., 2010) is visibly increased by MTSET modification (Figs. 4 D and 12 B; Po is 0.19 ± 0.04, $n = 5$ for cysless/M348C, and 0.63 ± 0.03, $n = 4$ for cysless/I344C). The single-channel trace of cysless/I344C in Fig. 12 B illustrates a negligible ATP-independent gating before MTSET modification, whereas frequent opening and closing events in the absence of ATP can be readily discerned after MTSET modification. Although the trace itself already demonstrates an increase of the opening rate after MTSET modification, kinetic analysis also reveals that the closing rate is decreased for ATP-independent gating (see legend to Fig. 12 for details).

The simplest hypothesis to explain the alterations of the stability of both the open and the closed states by MTS modification of engineered cysteines on one face of TM6 is that residues on this face interact with different parts of the CFTR protein in the open and closed states. In other words, this part of TM moves relatively to other TMs during gating transitions. Indeed, much previous work has suggested interactions of the cytoplasmic part of TM6 with other TMs. For example, biochemical studies demonstrated that both M348C and T351C can be cross-linked to T1142C in TM12 (Chen et al. 2004). R347 was shown to form a salt bridge with D924 in TM8 (Cotten and Welsh, 1999). More recently, it has also been suggested that R352 interacts with D993 in TM9 through an electrostatic mechanism (Cui et al., 2008; Jordan et al., 2008). In light of these reports, it would not be surprising if replacing hydrophobic side chains of I344 and M348 with cysteine thiolates plus MTSET adducts would alter their interactions. Likewise, depositing MTSET and MTSEA, two positively charged adducts with different chemical properties, into position 352 would lead to differential interactions.

Although more experiments are needed to reveal the exact motion of TM6 during the gating cycle, recent structural studies provide some clues. By comparing different crystal structures of ABC exporters including Sav1866, MsbA, and P-glycoprotein, Gutmann et al. (2010) proposed rotational movements of the transmembrane helices that form the substrate pathway as a molecular mechanism for switching the high-affinity, inward-facing conformation to a low-affinity, outward-facing conformation during a transport cycle. If this proposition is correct, the same mechanism may be used by members of ABCC subfamily that similarly export hydrophobic cargos out of the cell. Perhaps, as a member of the ABCC subfamily, CFTR may adopt this molecular motion for opening and closing of the gate.

Roles of TM6 in the formation of the CFTR pore

Although the current study provides compelling evidence for the involvement of TM6 in gating motion, its role on anion permeation is less straightforward. On the one hand, several of the current results are consistent with the idea that TM6 lines the pore. First, similar to previous findings (Tabcharani et al., 1993; McDonough et al., 1994; Linsdell et al. 1998, 2000; Smith et al., 2001; Cui et al., 2008), mutations at seven positions (Fig. 2) decrease the single-channel amplitude. Second, the potency to an open-channel blocker, glibenclamide, is reduced by the charge-neutralizing mutation R352C (also see Cui et al., 2008), but was restored by charge-restoring

modification (Fig. 8). Third, negatively charged MTS reagents inhibit anion flow as reflected in the reduced single-channel amplitude after modification (Figs. 9 and 10). However, although these functional results when considered as a whole do support the role of TM6 in deciding the pore properties, data from each individual approach may not be sufficient to substantiate the hypothesis that the targeted residue(s) lines the pore. One typical example is R347. This residue was first proposed to be a Cl^--binding site based on the loss of anomalous mole fraction effects with an R-to-D mutation (Tabcharani et al., 1993). But it is later shown that the mutation perturbs the gross pore architecture by disrupting the salt bridge formed by R347 and another residue in TM8 (Cotten and Welsh, 1999). Indeed, in the current study, R347C is insensitive to either MTSET or MTSES.

On the other hand, the results that MTSET modifications do not affect the single-channel amplitude (Figs. 5 and 6) are at odds with the picture that these positions directly face the pore. It seems hard to envision that chloride conduction through a narrow pore is not affected by placing a bulky, positively charged side chain in the pore. In comparison, it has been shown previously that cysteine modification by either MTSES or MTSET inhibits ion flow through the ClC-0 Cl^- channel (Lin and Chen, 2003). One may argue that this lack of effect on the single-channel amplitude by MTSET modification is because the CFTR channel pore contains a deep, wide intracellular vestibule, the existence of which has long been considered in the field (Sheppard and Welsh, 1999; Dawson et al., 2003; Linsdell, 2006). If we assume that the cytoplasmic part of TM6 lines the wall of a wide internal vestibule, the dramatic effects on channel permeation induced by the negatively charged MTSES can be attributed to the unfavorable electrostatic interaction between the negatively charged adducts and Cl^-. This assumption also implicates that the large intracellular vestibule ensures that the bulky MTS adducts (both MTSES and MTSET are ~6 Å in diameter; Karlin and Akabas, 1998) do not sterically hinder anion conduction. Thus, adding a positively charged adduct in this vestibule by MTSET modification only poses minor effects on anion conduction. This picture, however, is still incompatible with our results showing slow modification rates for 344C and 345C, which suggest that they are not readily accessible and thus are probably not positioned in a wide aqueous environment. Furthermore, the steep voltage dependence for MTSES modification of 341C, 344C, and 345C also suggest that they are located in a narrow region deep in the membrane field.

The idea that TM6 lines the pore is nevertheless supported by recent homology models (Jordan et al., 2008; Mornon et al., 2008, 2009; Serohijos et al., 2008; Alexander et al., 2009) constructed using the crystal structure of ABC transporter Sav1866 (Dawson and Locher, 2006) as a template. At first glance, it seems reassuring that all six positive hits identified in the present study nicely snuggle on the surface of the ion permeation pathway in the homology models proposed by Serohijos et al. (2008) and Alexander et al. (2009). We are cautious here to point out several potential problems with these models. First, not surprisingly, all of these models show an outward-facing conformation of TMDs with the same gap separating two membrane-spanning halves of the molecule as seen in Sav1866 (Fig. 12 C). For Sav1866, this gap on the same plane as the outer leaflet of the membrane bilayer is probably essential for its function as a "vacuum cleaner" that moves hydrophobic substrates across the bilayer (see Gutmann et al., 2010 for details). In contrast, this space that is freely connected to the lipid bilayer is conceptually incompatible with the function of CFTR as an ion channel because ions and lipids simply don't mix. An ion channel pore needs to be guarded against the invasion of membrane lipids. Second, these outward-facing structural models show a pore widely open toward the external end with no apparent constriction beyond residue 352 (Fig. 12 C). This appears to be in conflict with the experimental data showing the existence of a barrier (residues 338–341) for the bulky MTS reagents. Third, close inspection of the pore from the cytoplasmic end of the modeled structures fails to observe a wide pore entrance that allows trespass by large organic anions that block the channel from the intracellular side of the membrane. Lastly, the idea that TM6 needs to interact with different parts of CFTR during gating transitions means that at least I344, M348, and R352 may not line the pore all the time. Thus, at this juncture, more studies are needed to elucidate the architecture of the CFTR pore.

We thank Cindy Chu for technical assistance.

This work was supported by National Institutes of Health (NIH) grants (NIHR01DK55835 and NIHR01HL53455). This investigation was conducted in a facility constructed with support from Research Facilities Improvement Program (grant C06 RR-016489-01) from the National Center for Research Resources, NIH.

Christopher Miller served as editor.

Submitted: 7 June 2010
Accepted: 11 August 2010

REFERENCES

Alexander, C., A. Ivetac, X. Liu, Y. Norimatsu, J.R. Serrano, A. Landstrom, M. Sansom, and D.C. Dawson. 2009. Cystic fibrosis transmembrane conductance regulator: using differential reactivity toward channel-permeant and channel-impermeant thiol-reactive probes to test a molecular model for the pore. *Biochemistry.* 48:10078–10088. doi:10.1021/bi901314c

Aubin, C.N., and P. Linsdell. 2006. Positive charges at the intracellular mouth of the pore regulate anion conduction in the CFTR chloride channel. *J. Gen. Physiol.* 128:535–545. doi:10.1085/jgp.200609516

Bear, C.E., C.H. Li, N. Kartner, R.J. Bridges, T.J. Jensen, M. Ramjeesingh, and J.R. Riordan. 1992. Purification and functional reconstitution of the cystic fibrosis transmembrane conductance regulator (CFTR). *Cell.* 68:809–818. doi:10.1016/0092-8674(92)90155-6

Beck, E.J., Y. Yang, S. Yaemsiri, and V. Raghuram. 2008. Conformational changes in a pore-lining helix coupled to cystic fibrosis transmembrane conductance regulator channel gating. *J. Biol. Chem.* 283:4957–4966. doi:10.1074/jbc.M702235200

Bompadre, S.G., T. Ai, J.H. Cho, X. Wang, Y. Sohma, M. Li, and T.C. Hwang. 2005. CFTR gating I. Characterization of the ATP-dependent gating of a phosphorylation-independent CFTR channel (DeltaR-CFTR). *J. Gen. Physiol.* 125:361–375. doi:10.1085/jgp.200409227

Bompadre, S.G., Y. Sohma, M. Li, and T.C. Hwang. 2007. G551D and G1349D, two CF-associated mutations in the signature sequences of CFTR, exhibit distinct gating defects. *J. Gen. Physiol.* 129:285–298. doi:10.1085/jgp.200609667

Chen, E.Y., M.C. Bartlett, T.W. Loo, and D.M. Clarke. 2004. The DeltaF508 mutation disrupts packing of the transmembrane segments of the cystic fibrosis transmembrane conductance regulator. *J. Biol. Chem.* 279:39620–39627. doi:10.1074/jbc.M407887200

Chen, T.Y., and T.C. Hwang. 2008. CLC-0 and CFTR: chloride channels evolved from transporters. *Physiol. Rev.* 88:351–387. doi:10.1152/physrev.00058.2006

Cotten, J.F., and M.J. Welsh. 1999. Cystic fibrosis-associated mutations at arginine 347 alter the pore architecture of CFTR. Evidence for disruption of a salt bridge. *J. Biol. Chem.* 274:5429–5435. doi:10.1074/jbc.274.9.5429

Csanády, L. 2000. Rapid kinetic analysis of multichannel records by a simultaneous fit to all dwell-time histograms. *Biophys. J.* 78:785–799. doi:10.1016/S0006-3495(00)76636-7

Csanády, L., P. Vergani, and D.C. Gadsby. 2010. Strict coupling between CFTR's catalytic cycle and gating of its Cl− ion pore revealed by distributions of open channel burst durations. *Proc. Natl. Acad. Sci. USA.* 107:1241–1246. doi:10.1073/pnas.0911061107

Cui, G., Z.R. Zhang, A.R. O'Brien, B. Song, and N.A. McCarty. 2008. Mutations at arginine 352 alter the pore architecture of CFTR. *J. Membr. Biol.* 222:91–106. doi:10.1007/s00232-008-9105-9

Cui, L., L. Aleksandrov, Y.X. Hou, M. Gentzsch, J.H. Chen, J.R. Riordan, and A.A. Aleksandrov. 2006. The role of cystic fibrosis transmembrane conductance regulator phenylalanine 508 side chain in ion channel gating. *J. Physiol.* 572:347–358. doi:10.1113/jphysiol.2005.099457

Dawson, R.J., and K.P. Locher. 2006. Structure of a bacterial multidrug ABC transporter. *Nature.* 443:180–185. doi:10.1038/nature05155

Dawson, D.C., X. Liu, Z.R. Zhang, and N.A. McCarty. 2003. Anion conduction by CFTR: mechanisms and models. *In* The Cystic Fibrosis Transmembrane Conductance Regulator. K.L. Kirk and D.C. Dawson, editors. Plenum Publishers, New York. 1–34.

Engh, A.M., and M. Maduke. 2005. Cysteine accessibility in ClC-0 supports conservation of the ClC intracellular vestibule. *J. Gen. Physiol.* 125:601–617. doi:10.1085/jgp.200509258

Fatehi, M., and P. Linsdell. 2008. State-dependent access of anions to the cystic fibrosis transmembrane conductance regulator chloride channel pore. *J. Biol. Chem.* 283:6102–6109. doi:10.1074/jbc.M707736200

Gadsby, D.C., P. Vergani, and L. Csanády. 2006. The ABC protein turned chloride channel whose failure causes cystic fibrosis. *Nature.* 440:477–483. doi:10.1038/nature04712

Gutmann, D.A., A. Ward, I.L. Urbatsch, G. Chang, and H.W. van Veen. 2010. Understanding polyspecificity of multidrug ABC transporters: closing in on the gaps in ABCB1. *Trends Biochem. Sci.* 35:36–42. doi:10.1016/j.tibs.2009.07.009

Higgins, C.F., and K.J. Linton. 2004. The ATP switch model for ABC transporters. *Nat. Struct. Mol. Biol.* 11:918–926. doi:10.1038/nsmb836

Hwang, T.C., and D.N. Sheppard. 2009. Gating of the CFTR Cl− channel by ATP-driven nucleotide-binding domain dimerisation. *J. Physiol.* 587:2151–2161. doi:10.1113/jphysiol.2009.171595

Jordan, I.K., K.C. Kota, G. Cui, C.H. Thompson, and N.A. McCarty. 2008. Evolutionary and functional divergence between the cystic fibrosis transmembrane conductance regulator and related ATP-binding cassette transporters. *Proc. Natl. Acad. Sci. USA.* 105:18865–18870. doi:10.1073/pnas.0806306105

Karlin, A., and M.H. Akabas. 1998. Substituted-cysteine accessibility method. *Methods Enzymol.* 293:123–145. doi:10.1016/S0076-6879(98)93011-7

Khare, D., M.L. Oldham, C. Orelle, A.L. Davidson, and J. Chen. 2009. Alternating access in maltose transporter mediated by rigid-body rotations. *Mol. Cell.* 33:528–536. doi:10.1016/j.molcel.2009.01.035

Kogan, I., M. Ramjeesingh, L.J. Huan, Y. Wang, and C.E. Bear. 2001. Perturbation of the pore of the cystic fibrosis transmembrane conductance regulator (CFTR) inhibits its atpase activity. *J. Biol. Chem.* 276:11575–11581. doi:10.1074/jbc.M010403200

Li, M., T.H. Chang, S.D. Silberberg, and K.J. Swartz. 2008. Gating the pore of P2X receptor channels. *Nat. Neurosci.* 11:883–887. doi:10.1038/nn.2151

Li, Y., W.P. Yu, C.W. Lin, and T.Y. Chen. 2005. Oxidation and reduction control of the inactivation gating of Torpedo ClC-0 chloride channels. *Biophys. J.* 88:3936–3945. doi:10.1529/biophysj.104.055012

Lin, C.W., and T.Y. Chen. 2003. Probing the pore of ClC-0 by substituted cysteine accessibility method using methane thiosulfonate reagents. *J. Gen. Physiol.* 122:147–159. doi:10.1085/jgp.200308845

Linsdell, P. 2006. Mechanism of chloride permeation in the cystic fibrosis transmembrane conductance regulator chloride channel. *Exp. Physiol.* 91:123–129. doi:10.1113/expphysiol.2005.031757

Linsdell, P., S.X. Zheng, and J.W. Hanrahan. 1998. Non-pore lining amino acid side chains influence anion selectivity of the human CFTR Cl− channel expressed in mammalian cell lines. *J. Physiol.* 512:1–16. doi:10.1111/j.1469-7793.1998.001bf.x

Linsdell, P., A. Evagelidis, and J.W. Hanrahan. 2000. Molecular determinants of anion selectivity in the cystic fibrosis transmembrane conductance regulator chloride channel pore. *Biophys. J.* 78:2973–2982. doi:10.1016/S0006-3495(00)76836-6

Liu, X., Z.R. Zhang, M.D. Fuller, J. Billingsley, N.A. McCarty, and D.C. Dawson. 2004. CFTR: a cysteine at position 338 in TM6 senses a positive electrostatic potential in the pore. *Biophys. J.* 87:3826–3841. doi:10.1529/biophysj.104.050534

Liu, X., C. Alexander, J. Serrano, E. Borg, and D.C. Dawson. 2006. Variable reactivity of an engineered cysteine at position 338 in cystic fibrosis transmembrane conductance regulator reflects different chemical states of the thiol. *J. Biol. Chem.* 281:8275–8285. doi:10.1074/jbc.M512458200

Liu, Y., M. Holmgren, M.E. Jurman, and G. Yellen. 1997. Gated access to the pore of a voltage-dependent K+ channel. *Neuron.* 19:175–184. doi:10.1016/S0896-6273(00)80357-8

Locher, K.P. 2009. Structure and mechanism of ATP-binding cassette transporters. *Philos. Trans. R. Soc. Lond. B Biol. Sci.* 364:239–245. doi:10.1098/rstb.2008.0125

Luo, J., M.D. Pato, J.R. Riordan, and J.W. Hanrahan. 1998. Differential regulation of single CFTR channels by PP2C, PP2A, and other phosphatases. *Am. J. Physiol.* 274:C1397–C1410.

Ma, T., J.R. Thiagarajah, H. Yang, N.D. Sonawane, C. Folli, L.J. Galietta, and A.S. Verkman. 2002. Thiazolidinone CFTR inhibitor identified by high-throughput screening blocks cholera toxin-induced intestinal fluid secretion. *J. Clin. Invest.* 110:1651–1658.

Mansoura, M.K., S.S. Smith, A.D. Choi, N.W. Richards, T.V. Strong, M.L. Drumm, F.S. Collins, and D.C. Dawson. 1998.

Cystic fibrosis transmembrane conductance regulator (CFTR) anion binding as a probe of the pore. *Biophys. J.* 74:1320–1332. doi:10.1016/S0006-3495(98)77845-2

McCarty, N.A. 2000. Permeation through the CFTR chloride channel. *J. Exp. Biol.* 203:1947–1962.

McCarty, N.A., and Z.R. Zhang. 2001. Identification of a region of strong discrimination in the pore of CFTR. *Am. J. Physiol. Lung Cell. Mol. Physiol.* 281:L852–L867.

McDonough, S., N. Davidson, H.A. Lester, and N.A. McCarty. 1994. Novel pore-lining residues in CFTR that govern permeation and open-channel block. *Neuron.* 13:623–634. doi:10.1016/0896-6273(94)90030-2

Mense, M., P. Vergani, D.M. White, G. Altberg, A.C. Nairn, and D.C. Gadsby. 2006. In vivo phosphorylation of CFTR promotes formation of a nucleotide-binding domain heterodimer. *EMBO J.* 25:4728–4739. doi:10.1038/sj.emboj.7601373

Mornon, J.P., P. Lehn, and I. Callebaut. 2008. Atomic model of human cystic fibrosis transmembrane conductance regulator: membrane-spanning domains and coupling interfaces. *Cell. Mol. Life Sci.* 65:2594–2612. doi:10.1007/s00018-008-8249-1

Mornon, J.P., P. Lehn, and I. Callebaut. 2009. Molecular models of the open and closed states of the whole human CFTR protein. *Cell. Mol. Life Sci.* 66:3469–3486. doi:10.1007/s00018-009-0133-0

Rees, D.C., E. Johnson, and O. Lewinson. 2009. ABC transporters: the power to change. *Nat. Rev. Mol. Cell Biol.* 10:218–227. doi:10.1038/nrm2646

Reyes, N., and D.C. Gadsby. 2006. Ion permeation through the Na+,K+-ATPase. *Nature.* 443:470–474. doi:10.1038/nature05129

Riordan, J.R., J.M. Rommens, B. Kerem, N. Alon, R. Rozmahel, Z. Grzelczak, J. Zielenski, S. Lok, N. Plavsic, J.L. Chou, et al. 1989. Identification of the cystic fibrosis gene: cloning and characterization of complementary DNA. *Science.* 245:1066–1073. doi:10.1126/science.2475911

Serohijos, A.W., T. Hegedus, A.A. Aleksandrov, L. He, L. Cui, N.V. Dokholyan, and J.R. Riordan. 2008. Phenylalanine-508 mediates a cytoplasmic-membrane domain contact in the CFTR 3D structure crucial to assembly and channel function. *Proc. Natl. Acad. Sci. USA.* 105:3256–3261. doi:10.1073/pnas.0800254105

Sheppard, D.N., and K.A. Robinson. 1997. Mechanism of glibenclamide inhibition of cystic fibrosis transmembrane conductance regulator Cl− channels expressed in a murine cell line. *J. Physiol.* 503:333–346. doi:10.1111/j.1469-7793.1997.333bh.x

Sheppard, D.N., and M.J. Welsh. 1999. Structure and function of the CFTR chloride channel. *Physiol. Rev.* 79:S23–S45.

Smith, S.S., X. Liu, Z.R. Zhang, F. Sun, T.E. Kriewall, N.A. McCarty, and D.C. Dawson. 2001. CFTR: covalent and noncovalent modification suggests a role for fixed charges in anion conduction. *J. Gen. Physiol.* 118:407–431. doi:10.1085/jgp.118.4.407

Tabcharani, J.A., J.M. Rommens, Y.X. Hou, X.B. Chang, L.C. Tsui, J.R. Riordan, and J.W. Hanrahan. 1993. Multi-ion pore behaviour in the CFTR chloride channel. *Nature.* 366:79–82. doi:10.1038/366079a0

Tsai, M.F., H. Shimizu, Y. Sohma, M. Li, and T.C. Hwang. 2009. State-dependent modulation of CFTR gating by pyrophosphate. *J. Gen. Physiol.* 133:405–419. doi:10.1085/jgp.200810186

Tsai, M.F., M. Li, and T.C. Hwang. 2010. Stable ATP binding mediated by a partial NBD dimer of the CFTR chloride channel. *J. Gen. Physiol.* 135:399–414. doi:10.1085/jgp.201010399

Vergani, P., S.W. Lockless, A.C. Nairn, and D.C. Gadsby. 2005. CFTR channel opening by ATP-driven tight dimerization of its nucleotide-binding domains. *Nature.* 433:876–880. doi:10.1038/nature03313

Wang, W., J. Wu, K. Bernard, G. Li, G. Wang, M.O. Bevensee, and K.L. Kirk. 2010. ATP-independent CFTR channel gating and allosteric modulation by phosphorylation. *Proc. Natl. Acad. Sci. USA.* 107:3888–3893. doi:10.1073/pnas.0913001107

Wang, Y., T.W. Loo, M.C. Bartlett, and D.M. Clarke. 2007. Correctors promote maturation of cystic fibrosis transmembrane conductance regulator (CFTR)-processing mutants by binding to the protein. *J. Biol. Chem.* 282:33247–33251. doi:10.1074/jbc.C700175200

Ward, A., C.L. Reyes, J. Yu, C.B. Roth, and G. Chang. 2007. Flexibility in the ABC transporter MsbA: alternating access with a twist. *Proc. Natl. Acad. Sci. USA.* 104:19005–19010. doi:10.1073/pnas.0709388104

Wilson, G.G., and A. Karlin. 1998. The location of the gate in the acetylcholine receptor channel. *Neuron.* 20:1269–1281. doi:10.1016/S0896-6273(00)80506-1

Zhang, Z.R., B. Song, and N.A. McCarty. 2005. State-dependent chemical reactivity of an engineered cysteine reveals conformational changes in the outer vestibule of the cystic fibrosis transmembrane conductance regulator. *J. Biol. Chem.* 280:41997–42003. doi:10.1074/jbc.M510242200

Zhou, J.J., M.S. Li, J. Qi, and P. Linsdell. 2010. Regulation of conductance by the number of fixed positive charges in the intracellular vestibule of the CFTR chloride channel pore. *J. Gen. Physiol.* 135:229–245. doi:10.1085/jgp.200910327

Zhou, Z., S. Hu, and T.C. Hwang. 2002. Probing an open CFTR pore with organic anion blockers. *J. Gen. Physiol.* 120:647–662.

Zhou, Z., X. Wang, H.Y. Liu, X. Zou, M. Li, and T.C. Hwang. 2006. The two ATP binding sites of cystic fibrosis transmembrane conductance regulator (CFTR) play distinct roles in gating kinetics and energetics. *J. Gen. Physiol.* 128:413–422. doi:10.1085/jgp.200609622

Zhu, T., D. Dahan, A. Evagelidis, S. Zheng, J. Luo, and J.W. Hanrahan. 1999. Association of cystic fibrosis transmembrane conductance regulator and protein phosphatase 2C. *J. Biol. Chem.* 274:29102–29107. doi:10.1074/jbc.274.41.29102